

Robotic Exploration of Unknown 2D Environment Using a Frontier-based Automatic-Differentiable Information Gain Measure

Di Deng, Runlin Duan, Jiahong Liu, Kuangjie Sheng, and Kenji Shimada

Abstract—At the heart of path-planning methods for autonomous robotic exploration is a heuristic which encourages exploring unknown regions of the environment. Such heuristics are typically computed using frontier-based or information-theoretic methods. Frontier-based methods define the information gain of an exploration path as the number of boundary cells, or frontiers, which are visible from the path. However, the discrete and non-differentiable nature of this measure of information gain makes it difficult to optimize using gradient-based methods. In contrast, information-theoretic methods define information gain as the mutual information between the sensor’s measurements and the explored map. However, computation of the gradient of mutual information involves finite differencing and is thus computationally expensive. In this work, we propose an exploration planning framework which combines sampling-based path planning and gradient-based path optimization. The main contribution of this framework is a novel reformulation of information gain as a differentiable function. This allows us to simultaneously optimize information gain with other differentiable quality measures, such as smoothness. The effectiveness of the proposed planning framework is verified both in simulation and in hardware experiments using a Turtlebot3 Burger robot.

I. INTRODUCTION

There has been an increasing demand for exploring both indoor and outdoor areas using autonomous vehicles equipped with range sensors such as LIDARs and depth cameras. Typical applications of area exploration include search and surveillance, mapping, lawn mowing, floor cleaning, etc. These applications require robots that generate paths automatically covering bounded regions based on onboard sensor readings. Fig. 1 shows an area exploration task for exploring an indoor environment with a Turtlebot3 Burger robot.

To explore an unknown region, the region is typically represented as a probabilistic occupancy map containing cells. The probability of each cell represents whether the cell is unknown, free, or occupied. As the robot explores the region, the occupancy probability is updated with the robot’s sensor measurements.

Guiding the robot to exhaustively and efficiently cover the entire unknown space is most commonly carried out in a receding-horizon fashion: the robot plans a path, follows the path, updates the map with the sensor data collected along the path, and repeats this process until the region is fully explored [1]. Existing approaches typically search for exploration paths using a collision-free path planner [2], and then try to optimize the information gain of an exploration

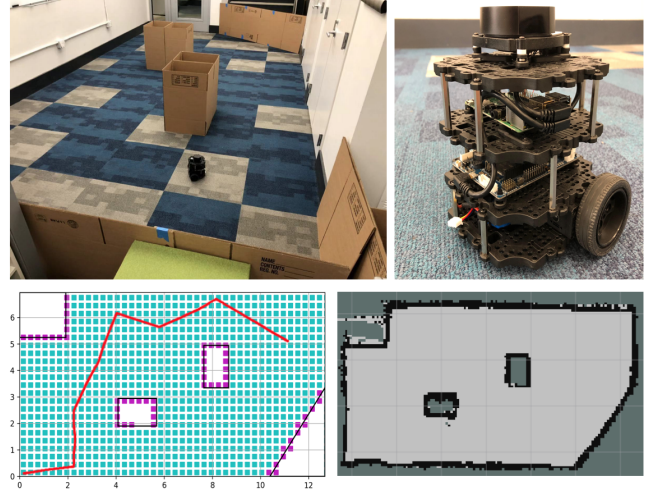


Fig. 1: Path planning for area coverage with a LIDAR-equipped robot.

path by finding the view-point that is most likely to maximize exploring unknown regions [3]–[5]. Two main approaches have been proposed to quantify the information gain of a path: (i) frontier-based [6], [7] and (ii) information-theoretic methods [8]–[10].

Frontier-based methods measure information gain by counting the number of boundary cells observable from the path. As it is a non-differentiable function of the path, the optimization of information gain is typically achieved by computing the information gain for a finite number of samples and choosing one with the largest information gain.

On the other hand, information-theoretic methods are designed to optimize an objective function such as mutual information or Shannon’s entropy [11], [12]. However, information-theoretic methods such as [13] denote information gain as a function of a discrete set of robot positions and compute gradients using finite differences. Both metrics are computationally expensive, limiting the replanning frequency of a robot during exploration.

Contribution. We introduce a novel algorithm for the exploration problem with a robot for area exploration tasks. The proposed approach reformulates a frontier-based information gain measure as an automatic-differentiable function with respect to the robot’s path, allowing the path to be optimized with gradient-based optimization. In contrast, traditional frontier-based methods typically optimize information gain by sampling a large number of paths. In addition, compared with information-theoretic methods, gradient computed with

the proposed automatic differentiation approach has higher accuracy and less computational complexity.

II. RELATED WORK

Frontier-based methods. Connolly defines frontiers as the region which separates the free space and unexplored regions of a grid map and evaluates the information gain of a view-point as the number of frontier cells visible from a view-point [14]. The straightforward use of frontiers to encourage exploration is to navigate a robot directly to the frontier cells [15]. Freda *et al.* [16] use a frontier-based modification of the Sensor-based Random Tree (SRT) method that only samples configurations within a maximum collision-free circular or star-shaped local safe region around a robot. By deploying a probabilistic strategy, the randomly generated configurations are biased towards frontier regions. Dornhege *et al.* [17] proposed a more sophisticated strategy for information gain measurement by combining frontiers with void cells, which are defined as unknown cells within the convex hull of occupied cells.

Finding the view-point of the maximum information gain is known as the Next Best View (NBV) problem. This view-point is determined by sampling a significant number of candidate view-points, counting the frontier observed by each view-point, and selecting the one with the highest information gain [18]. Instead of searching a single view-point, Bircher *et al.* propose a receding-horizon approach that finds paths as the best branch in a rapidly exploring random tree (RRT) [2]. To extend from evaluating the vertices of the path, Song and Jo maximize information gain along the entire inspection path by iteratively reducing sampling range and employing the streaming set cover algorithm [3].

Information-theoretic methods maximize the mutual information between the discrete occupancy map and the future sensor's measurement. Julian *et al.* prove that by maximizing Shannon's mutual information [19], a robot is guaranteed to explore unknown space. However, Nelson and Michael [20] point out this approach limits the control frequency. To be computationally more efficient, Charrow *et al.* [21] utilize the Cauchy-Schwarz quadratic mutual information (CSQMI) [13] based on Renyi's quadratic entropy (RQE) [22] for selecting paths rather than destinations. CSQMI is substantially faster, but it is still computationally demanding due to the finite differences involved in computing the gradient of the mutual information.

Planning a path to the goal. After the aforementioned algorithms find a goal, a path from the robot's current configuration to the goal can be found by either a sampling-based method such as RRT [2], or a trajectory-optimization method [23], [24] such as CHOMP. Sampling-based methods have the advantage of achieving a feasible solution while avoiding local minima [25]; optimization-based approaches perform better at locally optimizing the information gain and path length.

III. OVERVIEW

The goal of the proposed planning framework is to explore an unknown bounded 2D region, $\mathbf{V} \subset \mathbb{R}^2$, with a ground robot

to determine the subsets of \mathbf{V} , which are free ($\mathbf{V}_{\text{free}} \subseteq \mathbf{V}$) and occupied ($\mathbf{V}_{\text{occ}} \subseteq \mathbf{V}$). Region \mathbf{V} is represented by a probabilistic occupancy grid map, $\mathbb{M}_{\text{prob}} \in \mathbb{R}^{m \times n}$, with cell resolution ϱ . The (i, j) entry of \mathbb{M}_{prob} , denoted by $\mathbb{M}_{\text{prob}}(i, j) \in [0, 1]$, is the probability of the cell at (i, j) being occupied, free, or unknown:

$$\mathbb{M}_{\text{prob}}(i, j) = \begin{cases} \text{free} & < 0.5 \\ \text{unknown} & = 0.5 \\ \text{occupied} & > 0.5 \end{cases} \quad (1)$$

The robot starts at an initial configuration, or view-point, denoted by $\xi_0 = [x, y, \theta]$. The planning framework is supposed to plan collision-free paths iteratively, $\Xi = \{\xi_0, \dots, \xi_n\}$, and use the sensor measurements along the paths to update \mathbb{M}_{prob} until the number of unknown cells becomes smaller than a specified threshold.

An overview of our optimization-based coverage planning framework is given in Fig. 2. The process starts from a collision-free initial position, perceives the environment using a 2D range sensor, and updates \mathbb{M}_{prob} accordingly. Then, a sampling-based NBV planner is adopted to generate a piecewise linear path within the explored free space, \mathbf{V}_{free} . The smoothness and information gain of the path generated by the sampling-based planner is then optimized using a differentiable objective function. These steps are executed repeatedly until a termination criterion is satisfied.

IV. PROBABILISTIC OCCUPANCY MAP

This section reviews the range sensor model and the classical probabilistic sensor fusion algorithm used in this paper.

A. 2D Range-Sensor Model

The range sensor shown in Fig. 3 has a maximum range R_{max} , beam aperture ω , and mean deviation error ϵ . The probability of whether a cell is occupied or free can be computed from range sensor measurements using the model proposed by Moravec and Elfes [26]:

$$O_r = \begin{cases} 1 - (\frac{\delta}{R - \epsilon})^2 & \delta \in [0, R - \epsilon] \\ (\frac{\delta - R}{\epsilon})^2 - 1 & \delta \in [R - \epsilon, R + \epsilon] \end{cases}, \quad (2)$$

$$O_a = 1 - (\frac{2\theta}{\omega})^2, \rho_O = \frac{1 + O_r(\delta)O_a(\theta)}{2}, \theta \in [-\frac{\omega}{2}, \frac{\omega}{2}], \quad (3)$$

where O_r , O_a and ρ_O are the distance, angle, and overall probability that a cell with distance δ along ray \mathbf{SP} is occupied.

B. Binary Bayes Filter (BBF)

BBF [27] updates its belief of whether each cell is empty, free, or unknown by fusing range sensor measurements, z_t , over time. Instead of directly dealing with probabilities, BBF uses the *log-odds* of probabilities, which is defined by:

$$\mathbb{M}_{\text{odds}} = \log \frac{\mathbb{M}_{\text{prob}}}{1 - \mathbb{M}_{\text{prob}}} \quad (4)$$

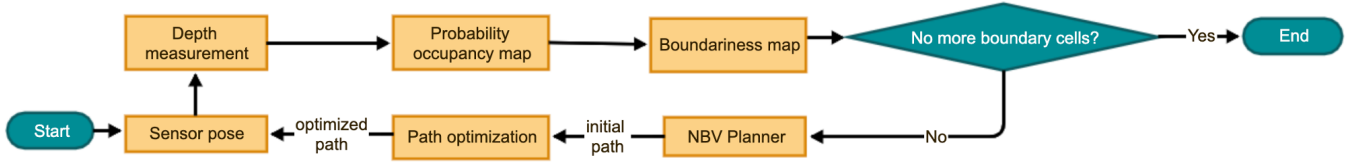


Fig. 2: Overview of the proposed optimization-based algorithm for coverage planning

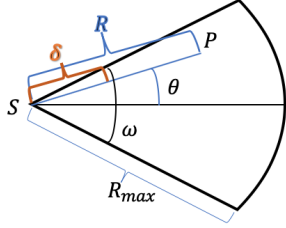


Fig. 3: Sensor model; R_{\max} is the maximum range measurement, ω is the beam aperture, S and P are the positions of sensor and obstacle, R is depth measurement, θ is the angle between the sensor's central axis and SP , and δ is the distance of a cell to sensor along SP .

such that:

$$\mathbb{M}_{\text{odds}}(i, j) = \begin{cases} < 0 & \text{free} \\ \log \frac{0.5}{1-0.5} = 0 & \text{unknown} \\ > 0 & \text{occupied} \end{cases} \quad (5)$$

Since there is a one-to-one mapping between probability and log-odds, the two representations of a probabilistic occupancy map are equivalent. The advantage of log-odds is that a Bayesian update can be implemented simply as the addition between the previous belief, $\mathbb{M}_{\text{prob}}(i, j|z_{1:t-1})$, and the update, $\mathbb{M}_{\text{odds}}(i, j|z_t)$. To improve numerical stability and adapt to dynamic environments with moving obstacles, upper and lower bounds, l_{\min} and l_{\max} , on log-odds are added during the updates [28]. The adjusted update rule is given by:

$$\mathbb{M}_{\text{odds}}(i, j|z_{1:t}) = \max(\min(\mathbb{M}_{\text{odds}}(i, j|z_{1:t-1}) + \mathbb{M}_{\text{odds}}(i, j|z_t), l_{\max}), l_{\min}). \quad (6)$$

V. BOUNDARINESS MAP

A *boundary* cell of a probabilistic occupancy map is classically defined as an unknown cell with at least one neighboring free cell. It represents the boundary between explored and unexplored regions and has been used as heuristics to guide exploration. For example, a common way to compute the information gain of a view-point, ξ , is to count the number of boundary cells observable by a robot at ξ [3]. Computer vision algorithms, such as edge detection, can also be applied to detect boundaries [15].

In this section, we define a numerical measure for cells called the *boundariness*. It is a number between 0 and 1. The closer a cell's boundariness is to 1, the more likely it is to be a boundary cell. The boundariness of Cell (i, j) is computed

from the log-odds of itself and its eight neighboring cells:

$$p = \sum_{(i,j) \in \mathbf{S}} \mathbb{M}_{\text{odds}}(i_0 + i, j_0 + j), \quad (7)$$

$$\mathbb{M}_{\text{bd}}(i_0, j_0) = w \exp \frac{-\mathbb{M}_{\text{odds}}(i_0, j_0)^2}{2\sigma^2} + (1-w) \exp \frac{-p^2}{2|\mathbf{S}|^2\sigma^2}, \quad (8)$$

where $\mathbf{S} = \{(\pm 1, \pm 1), (\pm 1, \mp 1), (\pm 1, 0), (0, \pm 1)\} \in \mathbb{R}^2$ is the set of relative indices of neighboring cells, and w a constant. The first term in Eqn. (8) rewards the fact that the cell is unknown. The second term is based on the observation that the cell is more likely to be a boundary if its neighboring cells contain a uniform mixture of occupied and free cells, e.g., four occupied and four free. Some examples of this heuristic are shown in Fig. 4.

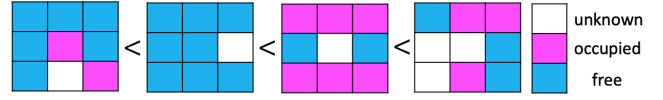


Fig. 4: Boundariness of the central cell computed from its neighbors.

However, several special cases need to be handled differently, as shown in Fig. 5.

- Left: when a cell is close to the edge of the occupancy map, it has less than eight neighbors.
- Middle: all known neighbors of a cell are occupied, then the cell is probably occluded. Its boundariness should be set to zero.
- Right: if all neighbors of a cell are unknown, the cell's boundariness should be set to zero.

Computing the boundariness of every cell in a probabilistic occupancy map, \mathbb{M}_{odds} , generates a boundariness map, $\mathbb{M}_{\text{bd}} \in \mathbb{R}^{m \times n}$. Examples of occupancy maps and their corresponding boundariness maps are shown in Fig. 6.

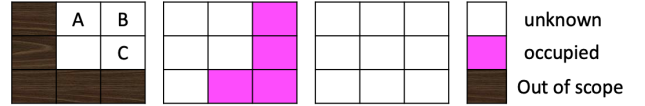


Fig. 5: Special conditions when calculating cell boundariness

VI. INFORMATION GAIN

Information gain is a measure of the number of boundary cells a view-point, ξ , or a sequence of view-points, Ξ , can observe. In many sampling-based exploration algorithms [1], [3], information gain is calculated by counting the number

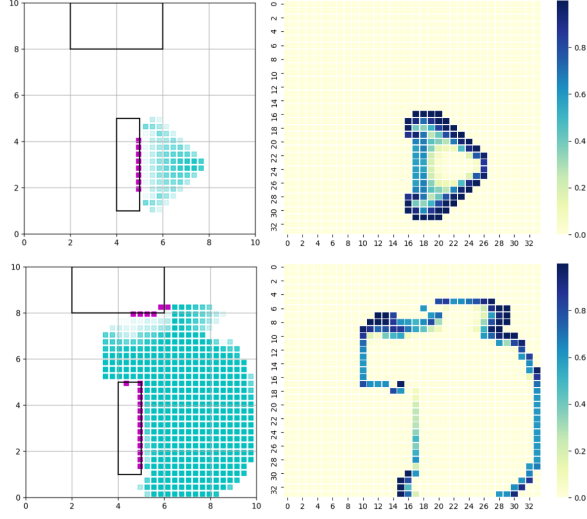


Fig. 6: Occupancy maps (left) and their corresponding boundariness maps (right). The darker the color, the higher the boundariness.

of boundary cells in the field of view of ξ or Ξ . However, this computation is fundamentally discrete and ill-suited for optimization. In this section, we propose differentiable information gain functions for single and multiple view-points, which will be used for gradient-based optimizations in later sections.

A. Fuzzy-Logic Filter

The fuzzy-logic filter for a view-point ξ , $\Phi_\xi : \Lambda(\xi) \rightarrow [0, 1]$, is a mapping from the set of cells surrounding ξ to a value between 0 and 1 that measures how far away each cell is from the field of view of view-point ξ . The fuzzy-logic filter for a path $\Xi = [\xi_0, \xi_1, \dots, \xi_k]$ can be defined analogously as $\Phi_\Xi : \Lambda(\Xi) \rightarrow [0, 1]$, where $\Lambda(\Xi)$ is a set of cells surrounding the path Ξ .

For a single view-point, $\xi = (x, y, \theta)$, $\Lambda(\xi)$ includes cells in a $4h \times 4h$ box with ξ at the center of the box, where $h = \frac{R_{\max}}{\varrho}$, and ϱ is the cell resolution. For Cell (i, j) in $\Lambda(\xi)$, its distance δ and direction v relative to ξ is calculated as:

$$\vec{V} = (i - 2h, j - 2h), \quad (9a)$$

$$\vec{v} = \vec{V} / \|\vec{V}\|_2, \quad (9b)$$

$$\delta = \varrho \|\vec{V}\|_2. \quad (9c)$$

The direction of the robot, \vec{u} , is given by $(\cos \theta, \sin \theta)$.

As shown in Fig. 7, the discount values are the highest when a cell is inside the field of view and drop linearly to zero as the cell gets further away. The expressions for the discount values for distance ϕ_d and angle ϕ_θ are:

$$\phi_d = \begin{cases} 0 & \delta > 2R_{\max} \\ \frac{2R_{\max} - \delta}{R_{\max}} & R_{\max} \leq \delta \leq 2R_{\max} \\ 1 & \delta < R_{\max} \end{cases}, \quad (10)$$

$$\phi_\theta = \begin{cases} \frac{1 + \vec{u} \cdot \vec{v}}{1 + \cos(\frac{\omega}{2})} & \vec{u} \cdot \vec{v} < \cos \frac{\omega}{2} \\ 1 & \vec{u} \cdot \vec{v} \geq \cos \frac{\omega}{2} \end{cases}. \quad (11)$$

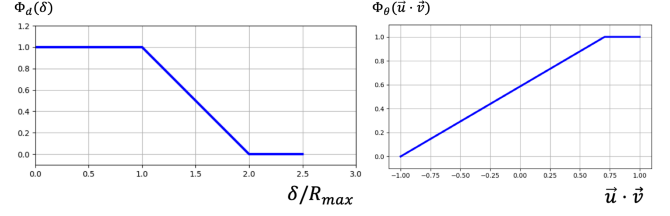


Fig. 7: Discount factors for the distance and the angle

Finally, the discount value of Cell (i, j) , $\Phi_\xi(i, j)$, is given as the product of the distance and angle discount values:

$$\Phi_\xi(i, j) = \phi_d(\delta) \phi_\theta(\vec{u}, \vec{v}, \omega). \quad (12)$$

For the sensor position shown in Fig. 8, the corresponding fuzzy-logic filter looks like the one shown in Fig. 9.

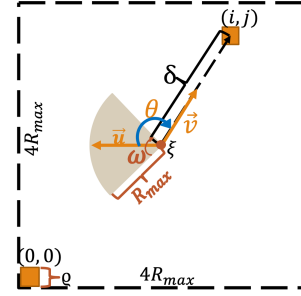


Fig. 8: Calculate discount factor; the size of the region is a square with edge distance $4R_{\max}$; shaded yellow area represents the robot's field of view; the distance and angle between sensor pose ξ and Cell (i, j) are δ and θ ; \vec{u} is the direction vector of the sensor, and \vec{v} is the vector from the sensor to Cell (i, j) .

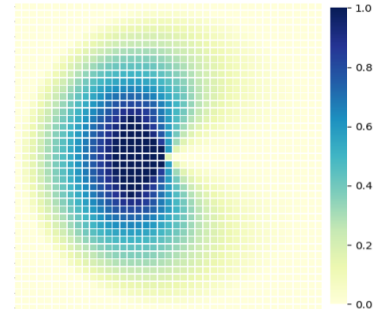


Fig. 9: Fuzzy-logic filter for camera position in Fig. 8

B. Information Gain for View-Point ξ

The information gain, IG, of a view-point, ξ , is a function of both ξ and the current boundariness map \mathbb{M}_{bd} , i.e., $\text{IG}_{\text{testview}}(\xi) : \mathbb{R}^3 \times \mathbb{R}^{m \times n} \rightarrow \mathbb{R}$. It sums over all cells in $\Lambda(\xi)$ the product of each cell's discount value and boundariness:

$$\text{IG}_{\text{view}}(\xi, \mathbb{M}_{\text{bd}}) = \sum_{(i_{\mathbb{M}}, j_{\mathbb{M}}) \in \Lambda(\xi)} \Phi(g(i_{\mathbb{M}}, j_{\mathbb{M}})) \mathbb{M}_{\text{bd}}(i_{\mathbb{M}}, j_{\mathbb{M}}), \quad (13)$$

where

$$(i, j) = g(i_M, j_M) = (i_M + 2h - \lfloor \frac{\xi[0]}{\varrho} \rfloor, j_M + 2h - \lfloor \frac{\xi[1]}{\varrho} \rfloor) \quad (14)$$

is the mapping from the boundary map index (i_M, j_M) to the fuzzy-logic filter index (i, j) .

C. Information Gain for Path Ξ

Algorithm 1 Calculate Information Gain for a Path

Input: Ξ, \mathbb{M}_{bd}

Output: $f(\Xi)$

- 1: $L = \sum_{i=0}^{k-1} \|\xi_{i+1} - \xi_i\|_2, N = \lceil \frac{L}{2\varrho} \rceil$
 - 2: **if** $k < N$ **then**
 - 3: $\Xi_s \leftarrow \text{Sample}(\Xi, N - k)$
 - 4: **end if**
 - 5: $\Xi = (\Xi \cup \Xi_s) \setminus \{\xi_0, \xi_k\}$
 - 6: $\Lambda(\Xi) = \bigcup_{\xi_i \in \Xi} \Lambda(\xi_i) \setminus \bigcup_{\xi_j \in \{\xi_0, \xi_k\}} \Lambda(\xi_j)$
 - 7: $f(\Xi) = \sum_{(i_M, j_M) \in \Lambda(\Xi)} \Phi_{\Xi}(i_M, j_M) \mathbb{M}_{bd}(i_M, j_M)$
-

Path Ξ is a collection of view-points: $\Xi = \{\xi_0, \xi_1, \dots, \xi_k\}$. Since the view regions of vertices in Ξ may overlap, we cannot compute the information gain of the path by directly summing information gains of individual vertices. Thus, we create a dynamic dictionary of fuzzy-logic filter Φ_{Ξ} for the path with (i_M, j_M) in Eqn. (14) as keys. This way, we can iteratively add or update the values in Φ_{Ξ} when calculating the fuzzy-logic filter for each view-point.

Alg. 1 shows the procedure of calculating the path information gain using Φ_{Ξ} . N in Line 2 is the expected number of view-points along a path with length L . If the total number of vertices in the path is less than N , we randomly sample $N - k$ points on the path in Line 5. As both the start and end points in the path are fixed, the goal is to maximize the boundary cells only covered by the intermediate view-points as shown in Lines 6 and 7. Similar to Eqn. (13), information gain of the path is calculated in Line 8.

VII. GRADIENT-BASED PATH OPTIMIZATION

This section introduces a gradient-based path optimization method which tries to improve Path Ξ 's smoothness and information gain simultaneously. A sampling-based method for creating an initial guess for the optimization is also introduced.

A. Objective Function

Given a path, $\Xi_0 = [\xi_0, \xi_1, \dots, \xi_k]$, we would like to improve both its smoothness and information gain by minimizing the following objective function:

$$f(\Xi) = \alpha \sum_{i=1}^k \|\xi_i - \xi_{i-1}\|_{\mathbf{W}}^2 - \text{IG}_{\text{path}}(\Xi, \mathbb{M}_{bd}). \quad (15)$$

The first term penalizes non-smoothness in the path. α is the weight of this term. $\|\cdot\|_{\mathbf{W}}$ represents the norm induced by symmetric positive definite matrix \mathbf{W} , i.e., $\|v\|_{\mathbf{W}}^2 = v^T \mathbf{W} v$. We choose $\mathbf{W} = \text{diag}([1, 1, 0.1])$ so that change in the

orientation, θ , is less costly compared to change in position, x and y . There is a minus sign before the path information gain, IG_{path} , because it is a quantity which we would like to maximize.

B. Initial Guess

The initial guess, $\Xi_0 = [\xi_0, \xi_1, \dots, \xi_k]$, is generated using RRT and then shortened with a common smoothing technique [2]. Our observation is that seeding the optimizer using a path generated by the sampling-based method helps the optimizer avoid local minima and achieve more complete coverage. The starting view-point, ξ_0 , is simply the current configuration of the robot. The goal view-point, ξ_k , is vital for guiding the exploration so that we will elaborate on the goal-selection method.

There are three requirements for selecting the goal, ξ_k : (1) ξ_k covers as many boundary cells as possible; (2) ξ_k does not get too close to obstacles; (3) the distance between ξ_0 and ξ_k is small. Accordingly, the scoring function, $f_{\text{score}} : \mathbb{R}^3 \times \mathbb{R}^{m \times n} \rightarrow \mathbb{R}$, which takes a view-point, ξ , and the current boundariness map, \mathbb{M}_{bd} , as its input and returns a scalar score, is defined as:

$$f_{\text{score}}(\xi, \mathbb{M}_{bd}) = \sum_{(i,j) \in \Lambda(\xi)} \mathbb{M}_{bd}(i,j) e^{-\lambda_1 \delta} e^{-\lambda_2 N_{\text{occupied}}}, \quad (16)$$

where $\Lambda(\xi)$ is the set of cells in the field of view of the robot at view-point ξ ; $\lambda_1, \lambda_2 \in (0, 1)$ are constant weights; $\delta = \|\xi_0 - \xi_k\|$; N_{occupied} is the number of obstacles in a user-defined box centered at ξ . The goal, ξ_k , is selected by sampling view-points on the entire grid, scoring them using the function in Eqn. (16), and picking the one with the highest score as ξ_k .

C. Results

The gradient of the differentiable objective function defined in Eqn. (15) can be evaluated using back-propagation [29]. Fig. 10 is an example of applying gradient descent to a path generated by a sampling-based planner. The gradient-based optimization reduces the path length from 3m to 1.95m and increases coverage by 15%.

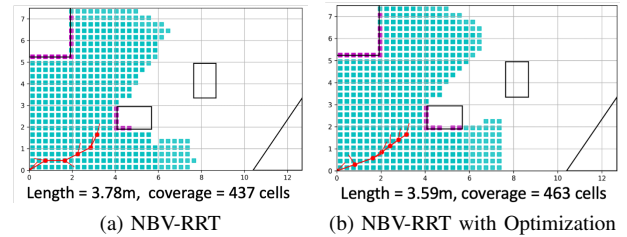


Fig. 10: Path optimization through a gradient descent method. Red dots with arrows represent the positions and orientations of the robot.

VIII. GRADIENT-BASED EXPLORATION

Alg. 2 is an overview of the gradient-based path planning algorithm to determine the occupancy map of the environment. The inputs to the system are: (1) the robot's initial configuration, ξ_0 , (2) the onboard sensor model with a maximum range of R_{\max} and a beam aperture of ω , (3) the dimension of the grid map (m, n) with cell resolution ϱ , and (4) the number of points to be sampled for goal selection N_s .

The log-odds map, \mathbb{M}_{odds} , and the boundariness map, \mathbb{M}_{bd} , are initialized as $m \times n$ matrices with all elements equal to zero. f_{Ξ} is defined as the information gains for τ_2 consecutive paths, and it is initialized as a list of $\mathbf{1}$ s with τ_2 elements. Line 2 updates both \mathbb{M}_{odds} and \mathbb{M}_{bd} based on the measurement from the initial configuration, ξ_0 . If the number of cells in \mathbb{M}_{bd} with probabilities of being at the boundary is greater than the constant threshold, τ_1 , and the summation of the information gains over the last τ_2 consecutive paths is greater than zero, we start to explore the environment.

Exploration path generation within the loop contains three main steps: (1) initial path generation with a greedy method with Lines 4 and 5; (2) path optimization through gradient descent in Line 6; (3) map revolution with a designed path from Line 8 to 11. Then in Line 12, we deploy the robot to the endpoint in the path and repeat the previous steps if all requirements in Line 3 are satisfied. After exploration, this algorithm calculates probability map \mathbb{M}_{prob} from log-odds map \mathbb{M}_{odds} to understand the distribution of obstacles and free space in the environment.

Algorithm 2 Gradient-Based Area Coverage

Input: $\xi_0, R_{\max}, \omega, m, n, \varrho, N_s$

Output: \mathbb{M}_{prob}

```

1:  $\mathbb{M}_{\text{odds}} = \mathbb{M}_{\text{bd}} = 0_{m,n}, f_{\Xi} = 1_{\tau_2}$ 
2:  $\mathbb{M}_{\text{odds}}, \mathbb{M}_{\text{bd}} \leftarrow \text{UpdateMap}(\xi_0, R_{\max}, \omega, \varrho, \mathbb{M}_{\text{odds}}, \mathbb{M}_{\text{bd}})$ 
3: while  $\text{size}(\mathbb{M}_{\text{bd}} > \rho) > \tau_1$  and  $\sum(f_{\Xi}) \neq 0$  do
4:    $\xi_{\text{goal}} \leftarrow \text{FindGoal}(\mathbb{M}_{\text{odds}}, \mathbb{M}_{\text{bd}}, N_s, R_{\max}, \omega, \varrho)$ 
5:    $\Xi \leftarrow \text{RRTPlanner}(\xi_0, \xi_{\text{goal}}, R_{\max}, \omega, \mathbb{M}_{\text{odds}}, \varrho)$ 
6:    $\Xi \leftarrow \text{GradientPlanner}(\Xi, \mathbb{M}_{\text{odds}}, \mathbb{M}_{\text{bd}})$ 
7:    $f_{\Xi} \leftarrow \text{UpdateInfoGain}(\Xi, \mathbb{M}_{\text{bd}}, \varrho, R_{\max})$ 
8:   for  $\xi \in \Xi$  do
9:      $\mathbb{M}_{\text{odds}}, \mathbb{M}_{\text{bd}} \leftarrow$ 
10:        $\text{UpdateMap}(\xi, R_{\max}, \omega, \varrho, \mathbb{M}_{\text{odds}}, \mathbb{M}_{\text{bd}})$ 
11:   end for
12:    $\xi_0 = \Xi[-1]$ 
13: end while
14:  $\mathbb{M}_{\text{prob}} \leftarrow \text{GetProbMap}(\mathbb{M}_{\text{odds}})$ 

```

IX. RESULTS AND DISCUSSION

Simulations and experiments with a Turtlebot3 Burger robot prove that our optimization algorithm improves area coverage and significantly reduces path length. As shown in Fig. 11, we compare the area coverage and path length before and after executing the optimization algorithm. After iteratively executing the proposed path optimization algorithm 21 times, the robot covers 98.5% of a region, consisting of 32×32

cells with a resolution of 0.3m. It has an average of 173% improvement of area coverage and 37% reduction of path length.

The log-odds upper and lower bounds used in the simulations are:

$$l_{\max} = \log \frac{0.9}{0.1}, l_{\min} = \log \frac{0.3}{0.7}. \quad (17)$$

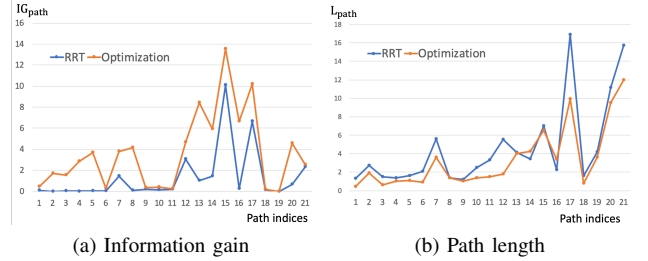


Fig. 11: Comparison between RRT and optimization

Our planner has consistent performance in different maps, as shown in Fig. 12. In these two cases, the lengths of paths are reduced by 43.7% and 40.9% without sacrificing the coverage area.

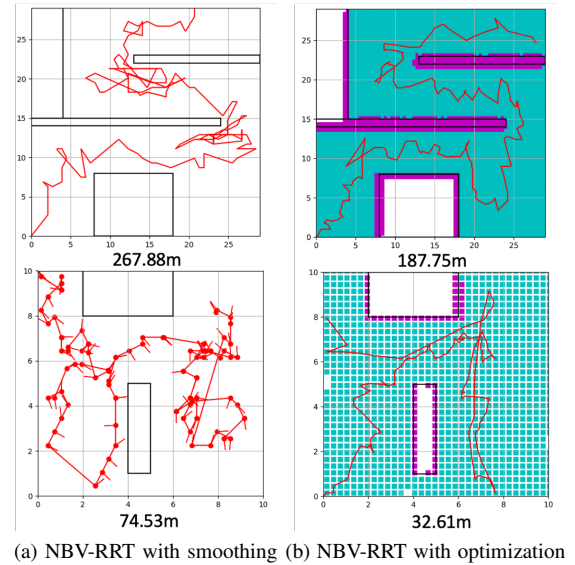


Fig. 12: Comparison of path lengths between RRT-smoothing algorithm and RRT-gradient descent algorithm

We then test our algorithm on a Turtlebot3 Burger robot in closed regions with a size of $6.5\text{m} \times 3.5\text{m}$ and $3.0\text{m} \times 3.5\text{m}$. The onboard 2D laser scanner has FOV (ω) of 90 degrees, maximum view range (R_{\max}) of 3m, and sensor resolution of 1° . The results shown in Fig. 13 demonstrate that our optimization-based planner generates relatively smooth paths and successfully covers the target regions.

X. CONCLUSIONS

We proposed a novel algorithm for the optimizing exploration paths of a robot to cover unknown 2D areas. This

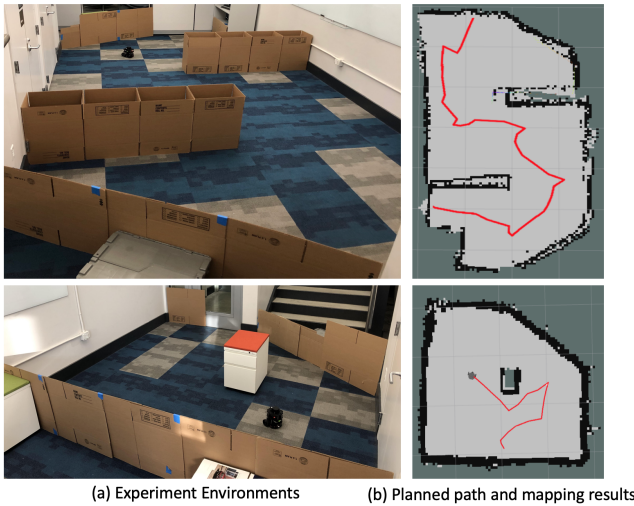


Fig. 13: Experiment results

algorithm starts with a path planned with the Next-Best-View algorithm, evaluates both the information gain of uniformly sampled view-points along the path, and then formulates a multi-objective utility function to maximize the coverage of boundary cells of these view-points through a gradient-descent method. To quantitatively measure the quality of the space being explored and assess a view-point's inspectability, we introduced a boundariness map, \mathbb{M}_{bd} , that estimates the likelihood of a cell being a boundary cell. Furthermore, the planner generates a path iteratively based on a pre-defined frequency to avoid unnecessary movements. Simulations and experimental results show that our algorithm improves area coverage while reducing path lengths.

ACKNOWLEDGEMENT

The authors would like to thank TOPRISE Co., LTD. for their financial support for this work.

REFERENCES

- [1] A. Bircher, M. Kamel, K. Alexis, H. Oleynikova, and R. Siegwart, "Receding horizon" next-best-view" planner for 3d exploration," in *2016 IEEE international conference on robotics and automation (ICRA)*. IEEE, 2016, pp. 1462–1468.
- [2] S. M. LaValle, *Planning algorithms*. Cambridge university press, 2006.
- [3] S. Song and S. Jo, "Online inspection path planning for autonomous 3d modeling using a micro-aerial vehicle," in *2017 IEEE International Conference on Robotics and Automation (ICRA)*. IEEE, 2017, pp. 6217–6224.
- [4] —, "Surface-based exploration for autonomous 3d modeling," in *2018 IEEE International Conference on Robotics and Automation (ICRA)*. IEEE, 2018, pp. 1–8.
- [5] P. S. Blaer and P. K. Allen, "Data acquisition and view planning for 3-d modeling tasks," in *2007 IEEE/RSJ International Conference on Intelligent Robots and Systems*. IEEE, 2007, pp. 417–422.
- [6] B. Yamauchi, "Frontier-based exploration using multiple robots," in *Proceedings of the second international conference on Autonomous agents*, 1998, pp. 47–53.
- [7] D. Holz, N. Basilico, F. Amigoni, and S. Behnke, "Evaluating the efficiency of frontier-based exploration strategies," in *ISR 2010 (41st International Symposium on Robotics) and ROBOTIK 2010 (6th German Conference on Robotics)*. VDE, 2010, pp. 1–8.
- [8] B. J. Julian, S. Karaman, and D. Rus, "On mutual information-based control of range sensing robots for mapping applications," *The International Journal of Robotics Research*, vol. 33, no. 10, pp. 1375–1392, 2014.
- [9] S. Bai, J. Wang, F. Chen, and B. Englot, "Information-theoretic exploration with bayesian optimization," in *2016 IEEE/RSJ International Conference on Intelligent Robots and Systems (IROS)*. IEEE, 2016, pp. 1816–1822.
- [10] F. Amigoni and V. Caglioti, "An information-based exploration strategy for environment mapping with mobile robots," *Robotics and Autonomous Systems*, vol. 58, no. 5, pp. 684–699, 2010.
- [11] F. Bourgault, A. A. Makarenko, S. B. Williams, B. Grocholsky, and H. F. Durrant-Whyte, "Information based adaptive robotic exploration," in *IEEE/RSJ international conference on intelligent robots and systems*, vol. 1. IEEE, 2002, pp. 540–545.
- [12] C. Stachniss, G. Grisetti, and W. Burgard, "Information gain-based exploration using rao-blackwellized particle filters," in *Robotics: Science and Systems*, vol. 2, 2005, pp. 65–72.
- [13] B. Charrow, G. Kahn, S. Patil, S. Liu, K. Goldberg, P. Abbeel, N. Michael, and V. Kumar, "Information-theoretic planning with trajectory optimization for dense 3d mapping," in *Robotics: Science and Systems*, vol. 11, 2015.
- [14] C. Connolly, "The determination of next best views," in *Proceedings. 1985 IEEE international conference on robotics and automation*, vol. 2. IEEE, 1985, pp. 432–435.
- [15] B. Yamauchi, "A frontier-based approach for autonomous exploration," in *cira*, vol. 97, 1997, p. 146.
- [16] L. Freda and G. Oriolo, "Frontier-based probabilistic strategies for sensor-based exploration," in *Proceedings of the 2005 IEEE International Conference on Robotics and Automation*. IEEE, 2005, pp. 3881–3887.
- [17] C. Dornhege and A. Kleiner, "A frontier-void-based approach for autonomous exploration in 3d," *Advanced Robotics*, vol. 27, no. 6, pp. 459–468, 2013.
- [18] A. Bircher, M. Kamel, K. Alexis, M. Burri, P. Oettershagen, S. Omari, T. Mantel, and R. Siegwart, "Three-dimensional coverage path planning via viewpoint resampling and tour optimization for aerial robots," *Autonomous Robots*, vol. 40, no. 6, pp. 1059–1078, 2016.
- [19] S. Verdu, "Fifty years of shannon theory," *IEEE Transactions on information theory*, vol. 44, no. 6, pp. 2057–2078, 1998.
- [20] E. Nelson and N. Michael, "Information-theoretic occupancy grid compression for high-speed information-based exploration," in *2015 IEEE/RSJ International Conference on Intelligent Robots and Systems (IROS)*. IEEE, 2015, pp. 4976–4982.
- [21] B. Charrow, S. Liu, V. Kumar, and N. Michael, "Information-theoretic mapping using cauchy-schwarz quadratic mutual information," in *2015 IEEE International Conference on Robotics and Automation (ICRA)*. IEEE, 2015, pp. 4791–4798.
- [22] A. Rényi, "Some fundamental questions of information theory," *Selected Papers of Alfred Renyi*, vol. 2, no. 174, pp. 526–552, 1976.
- [23] J. Schulman, J. Ho, A. X. Lee, I. Awwal, H. Bradlow, and P. Abbeel, "Finding locally optimal, collision-free trajectories with sequential convex optimization," in *Robotics: science and systems*, vol. 9, no. 1. Citeseer, 2013, pp. 1–10.
- [24] N. Ratliff, M. Zucker, J. A. Bagnell, and S. Srinivasa, "Chomp: Gradient optimization techniques for efficient motion planning," 2009.
- [25] G. A. Hollinger and G. S. Sukhatme, "Sampling-based robotic information gathering algorithms," *The International Journal of Robotics Research*, vol. 33, no. 9, pp. 1271–1287, 2014.
- [26] H. Moravec and A. Elfes, "High resolution maps from wide angle sonar," in *Proceedings. 1985 IEEE International Conference on Robotics and Automation*, vol. 2. IEEE, 1985, pp. 116–121.
- [27] S. Thrun, W. Burgard, and D. Fox, *Probabilistic robotics*. MIT press, 2005.
- [28] M. Yguel, O. Aycard, and C. Laugier, "Update policy of dense maps: Efficient algorithms and sparse representation," in *Field and Service Robotics*. Springer, 2008, pp. 23–33.
- [29] A. Griewank *et al.*, "On automatic differentiation," *Mathematical Programming: recent developments and applications*, vol. 6, no. 6, pp. 83–107, 1989.